Improving the acousto-optic detection of high-intensity focused ultrasound lesions

Matthew T. Adams, Qi Wang, Robin O. Cleveland, and Ronald A. Roy

Citation: Proc. Mtgs. Acoust. **19**, 075065 (2013); doi: 10.1121/1.4800271
View online: https://doi.org/10.1121/1.4800271
View Table of Contents: http://asa.scitation.org/toc/pma/19/1
Published by the Acoustical Society of America

Proceedings of Meetings on Acoustics

Volume 19, 2013 http://acousticalsociety.org/

ICA 2013 Montreal
Montreal, Canada
2 - 7 June 2013

Biomedical Acoustics
Session 3aBAb: Generation and Detection of High Intensity Focused Ultrasound Lesions

3aBAb4. Improving the acousto-optic detection of high-intensity focused ultrasound lesions

Matthew T. Adams*, Qi Wang, Robin O. Cleveland and Ronald A. Roy

***Corresponding author's address: Mechanical Engineering, Boston University, 110 Cummington Street, Boston, MA 02215, adamsm2@bu.edu**

Real-time acousto-optic (AO) sensing has been shown to non-invasively detect changes in ex vivo tissue optical properties during high-intensity focused ultrasound (HIFU) exposures. Although proof-of-concept experiments have been successful, the underlying parameters and mechanisms affecting the AO detectability of HIFU lesion formation are not well understood. In this work, a modeling based approach is used to improve the AO sensing of lesion formation during HIFU therapy. The angular spectrum method is used to model the acoustic field from the HIFU source and the temperature field, due to the absorption of ultrasound, is modeled using a finite-difference time-domain solution to the Pennes bioheat equation. Wavelength specific changes in tissue optical properties are calculated using a thermal dose model, calibrated by experimental data. The diffuse optical field is modeled using an open-source graphics processing unit accelerated Monte Carlo algorithm. The Monte Carlo algorithm is modified to account for light-sound interactions, using the acoustic field from the angular spectrum method, and to account for AO signal detection. Results will demonstrate the important roles of optical wavelength selection, and illumination and detection configurations on the detectability of HIFU lesions by optical and AO sensing methods. [Work supported in part by NSF].

Published by the Acoustical Society of America through the American Institute of Physics

 [DOI: 10.1121/1.4800271]
Received 22 Jan 2013; published 2 Jun 2013

INTRODUCTION

High-Intensity Focused Ultrasound (HIFU) is a non-invasive surgical technique where highly localized heating, caused by the absorption of focused ultrasound, results in irreversible tissue necrosis [1]. HIFU has been investigated for several therapeutic applications including the treatment of solid tumors in soft tissue such as breast [2, 3], prostate [4], and liver [5]. Although HIFU shows great promise, its development has been hindered by the treatment's unpredictability. Therapeutic results are dependent not only on exposure parameters, but also on environmentally specific factors such as blood flow, respiration, and variability in tissue properties which can be both patient and time dependent. Therefore, in order to improve the efficacy, safety, and clinical viability of HIFU, there is a need for reliable real-time monitoring techniques.

HIFU Treatment Monitoring

Although several non-invasive techniques have been investigated for monitoring HIFU treatments, only magnetic resonance imaging (MRI) [6] and diagnostic ultrasound imaging [7] have seen clinical use. Currently, MRI is considered the "gold standard" for HIFU guidance due to its ability to delineate between tissue types and monitor temperature changes with millimeter spatial resolution and 2°C temperature resolution [8]. However, there are significant disadvantages associated with MRI guidance - low temporal resolution, high cost, and the need for a magnetically compatible HIFU system - that have limited its accessibility and its widespread adoption [9]. Alternatively, diagnostic ultrasound guidance is comparatively inexpensive, portable, and capable of real-time imaging. However, due to the low acoustic contrast between normal and necrotic tissue, diagnostic ultrasound can only reliably guide HIFU treatments when the acoustic exposure generates boiling within the tissue [10].

Acousto-Optic Sensing of HIFU Lesions

The application of HIFU to soft tissue induces primary thermal injuries, such as the thermal dissociation of phospholipid cellular membranes and the thermal denaturation of intracellular and extracellular proteins, which can be detected immediately [11]. When proteins are thermally denatured, they are reduced from highly organized structures to small, amorphous granules of collapsed and ruptured amino acid chains, resulting in a large increase in the optical scattering and sometimes absorption coefficients of their host tissues [12, 13].

Acousto-Optic (AO) sensing is a dual-wave technique that uses a focused ultrasound field to phase modulate diffuse light in order to sense optical property changes in optically diffusive media, such as biological tissue, with the spatial resolution of ultrasound. Recently, Lai *et al.* [14] and Powell and Leung [15] have demonstrated real-time AO monitoring of HIFU lesion formation in *ex vivo* chicken breast samples using photo-refractive crystal based and autocorrelation detection techniques, respectively. Although these preliminary demonstrations have been successful, both systems are limited by their low signal-to-noise ratios (SNR). The low SNRs of the systems are due in part to the fact that the underlying parameters and mechanisms affecting the AO detectability of HIFU lesion formation are not well understood. In this work, a modeling based approach is used to enhance the efficacy of AO sensing of lesion formation during HIFU therapy.

Materials and Methods

To simulate the AO detection of HIFU lesion formation, several models have been developed and employed. Those models will be described in the following sections.

Acoustic Modeling

The three-dimensional pressure and intensity distribution from a HIFU source (H102-6, Sonic Concepts, WA) is modeled using the angular spectrum method in order to calculate ultrasonic heat deposition and acousto-optic phase modulations inside of insonified and illuminated tissue. The angular spectrum method makes use of 2-D FFT algorithms to expand an arbitrarily complex 2-D wave field into a series of plane waves. Each plane wave is then individually propagated to a parallel plane, where an inverse Fourier transform is used to revert the plane waves back to a complex 2-D field. In order to model the spherically curved surface of the HIFU source (70 mm aperture with a 20 mm diameter central hole, and a 62.4 mm focal length in water when driven at its 1.1 MHz center frequency) in a single plane, the Ring-Bessel technique was used [16]. The Ring-Bessel technique decomposes the curved source into circular rings of increasing radii, each ring a different distance from the front plane of the source, and calculates the angular spectrum of each ring.

Thermal Modeling

The temperature increase due to the absorption of ultrasound are modeled in three-dimensions using a Douglas-Rachford based finite difference time domain (FDTD) solution [17] to the Pennes bioheat transfer equation [18],

$$\rho C_v \frac{\partial T}{\partial t} - K\nabla^2 T = -W_b C_b (T - T_a) + 2\alpha I \tag{1}$$

Where ρ is mass density, C_v is specific heat capacity, T is tissue temperature, t is time, K is thermal conductivity, W_b is the blood perfusion coefficient of the tissue, C_b is the heat capacity of blood, T_a is the ambient blood temperature, α is the acoustic absorption coefficient, and I is the acoustic intensity.

Tissue that is thermally damaged is determined using the CEM_{43} thermal dose model [20]. During the thermal calculations, CEM_{43} is determined at every point in the tissue using the equation,

$$CEM_{43} = \int_{t=0}^{t_{final}} R^{43-T(t)} dt \tag{2}$$

Where $T(t)(^\circ\mathrm{C})$ is tissue temperature as a function of time, CEM_{43} is a measure of cumulative equivalent minutes spent at 43 °C, and the rate constant $R = 0.25$ if $T < 43\,^\circ\mathrm{C}$ and $R = 0.5$ if $T > 43\,^\circ\mathrm{C}$. It can be shown that if the thermal dose is known, the volume fraction of damaged tissue (F_d) can be calculated as [21],

$$F_d = 1 - \exp\left(-\frac{CEM_{43}}{D_0(43)}\right) \tag{3}$$

Where $D_0(43)$ is an empirical time constant.

Optical Modeling

To model light propagation inside of tissue, an open-source graphics processing unit (GPU) based Monte-Carlo code (MCX) is used [19]. The Monte-Carlo method is a stochastic technique

that simulates many individual photon "packets" in order to determine the overall fluence distribution inside of optically turbid media. MCX allows time-resolved simulations to be performed in an arbitrarily complex and heterogeneous voxel-based geometry, and supports the placement of detectors that record information from the photon packets that reach them.

To model optical property changes in response to denaturation, it is assumed that the optical properties are linearly proportional to the volume fraction of damaged tissue, F_d. Therefore, the thermal damage dependent optical properties $\mu_{thermal}$ are calculated as,

$$\mu_{thermal} = \mu_{normal} + F_d\left(\mu_{damaged} - \mu_{normal}\right) \tag{4}$$

Where μ_{normal} and $\mu_{damaged}$ are the optical properties of the normal and the fully damaged tissue.

Acousto-Optic Modeling

AO Monte-Carlo models have previously been developed for diffuse light in samples with heterogeneous optical parameters and a nonuniform ultrasound field, and have been implemented on both CPUs [22] and GPUs [23]. Much like their optical counterparts, these AO models simulate the propagation of individual photon packets. However, the simulations also track the phase shifts accumulated by the photons, due to the periodic displacement of optical scatterers and modulation of the tissue's refractive index, as they pass through the acoustic field. In this work, the open-source GPU-based Monte-Carlo model, MCX [19], is being modified to account for AO interactions and photorefractive crystal based detection. This work is currently ongoing.

Preliminary Results

Preliminary results are shown for a 40x40x40 mm chicken breast illuminated by a 1064 nm laser and insonified at 1.1 MHz for 15 seconds by an H102-6 HIFU transducer with an expected 6 MPa peak positive pressure in water. A cross-section (at $x = 0$) of the initial optical fluence and the acoustic pressure inside the sample are shown in Figure 1. The acoustic and optical properties used for this simulation are shown in Table 1.

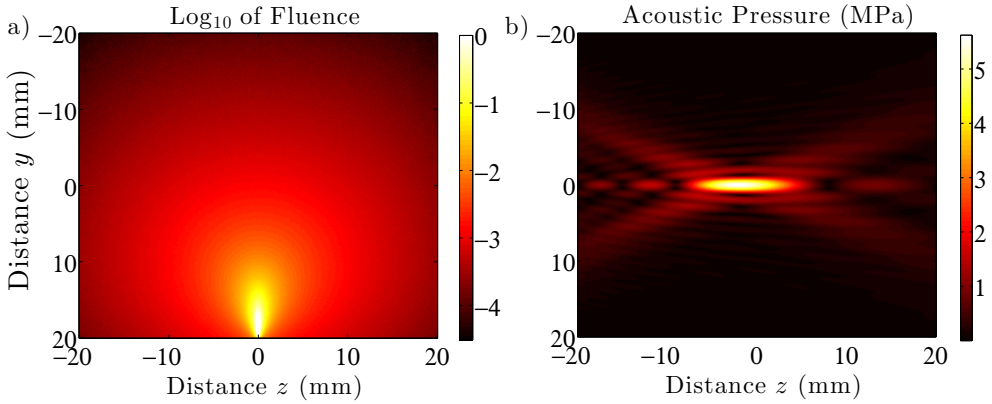

Figure 1: Exposure conditions for a typical AO-guided HIFU experiment. **a)** Optical fluence at $x = 0$ inside of a 40x40x40 mm chicken breast illuminated by a unity pencil beam directed along the y axis at $(0, 20, 0)$. **b)** Acoustic pressure at $x = 0$ inside of the same sample. A peak pressure of 6 MPa in water is targeted at the center of the sample $(0, 0, 0)$. The acoustic pressure propagates in the $+z$ direction.

TABLE 1: Acoustic and optical properties used for chicken breast.

Acoustic Property	Value	Optical Property	Value
c_0	1585 m/s	μ_s	30 cm^{-1}
ρ_0	1040 kg/m^3	μ_a	0.05 cm^{-1}
α	$5f^{1.1}$ Np/m/MHz	g	0.98

As the tissue absorbs the ultrasound, its temperature will increase according to Equation 1 and thermal damage will accumulate according to Equation 3. The increase in temperature and the resulting thermal dose from the exposure are shown in Figure 2. The tissue properties used for the thermal simulation are shown in Table 2. As thermal damage is accumulated in the HIFU focus, the optical properties of the tissue, and thus the optical fluence distribution will change.

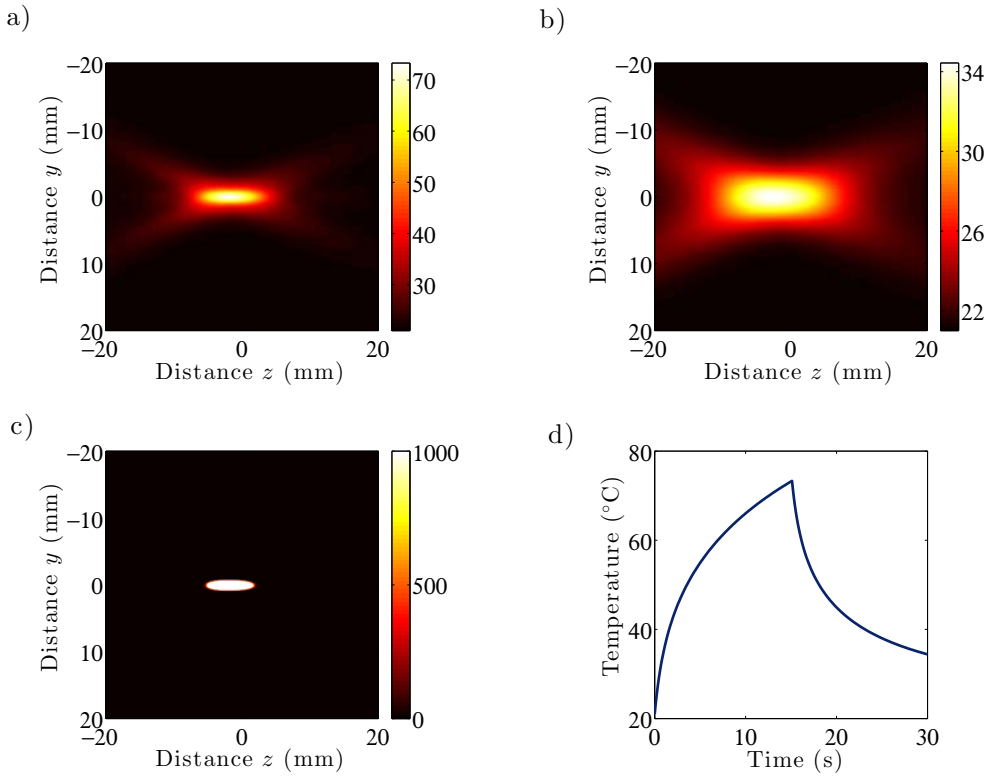

FIGURE 2: Temperature increase and thermal dose due to the absorption of ultrasound. Cooling due to perfusion is not considered. **a)** Temperature profile (°C) at t = 15s and x = 0. **b)** Temperature profile (°C) at t = 30s and x = 0. **c)** Thermal dose profile at t = 30s and x = 0. The plot is capped at 1000 cumulative equivalent minutes in order to illustrate the sharp lesion boundary. **d)** Temporal profile of the focal temperature.

TABLE 2: Thermal properties used for chicken breast.

Thermal Property	Value
C_v	3210 J/kg°C
K	0.4683 W/m°C
$T_{ambient}$	21°C

Discussion and Conclusions

When the tissue is illuminated by the pencil beam in Figure 1a, the light quickly becomes diffusive due to multiple scattering, thus demonstrating the need for AO sensing to enhance spatial resolution. The effects of the tissue on the acoustic field are less prominent, however it can be seen that the acoustic focus shifts about 2 mm towards the transducer and the peak pressure is attenuated by about 6.5%.

The thermal damage observed in Figure 2 is substantial enough to result in irreversible optical property changes that progress according to Equation 4. Visual observations of experimental results reveal that the boundary between normal and lesioned tissue is extremely sharp (on the order of 0.1 mm). This observation is also revealed in the thermal dose shown in Figure 2c. Accordingly, it is expected that the optical properties will feature a similarly sharp boundary between the normal and lesioned tissue. Experiments are currently underway to verify this result, and to study the relationship between temperature, thermal dose, and optical property changes.

As the optical properties of the tissue change as a function of thermal damage, so will the observed AO signals. Currently, the AO simulation described in this manuscript is still under development. Therefore, it is difficult to make any conclusions as to how the measured AO signal changes while the lesion develops. Once the AO model is completed, various illumination and detection configurations will be investigated to determine the optimal configuration for AO sensing of HIFU lesions.

Future Work

Future modeling work will focus on the modification of MCX to account for AO interactions and photorefractive crystal based detection. Additionally, experiments will be performed to investigate the relationship between thermal dose and optical properties with the goal of verifying current methods for modeling optical property changes in response to thermal denaturation. Once model development is completed, important parameters such as optical wavelength selection and illumination and detection configurations will be investigated to enhance the efficacy of AO sensing of lesion formation during HIFU therapy.

ACKNOWLEDGMENTS

The authors would like to thank David Giraud for his assistance with computational work, and the authors of MCX for access to their code and their helpful dialogue. This work is supported in part by the Boston University College of Engineering, and in part by the Gordon Center for Subsurface Sensing and Imaging Systems (NSF ERC Award No. EEC-9986821).

References

[1] G. Ter Haar, “Ultrasound focal beam surgery”, Ultrasound in medicine & biology **21**, 1089–1100 (1995).

[2] F. Wu, G. ter Haar, and W. Chen, “High-intensity focused ultrasound ablation of breast cancer”, Expert review of anticancer therapy **7**, 823–831 (2007).

[3] A. Schmitz, D. Gianfelice, B. Daniel, W. Mali, and M. van den Bosch, “Image-guided focused ultrasound ablation of breast cancer: current status, challenges, and future directions”, European radiology **18**, 1431–1441 (2008).

[4] A. Gelet, J. Chapelon, R. Bouvier, O. Rouviere, Y. Lasne, D. Lyonnet, and J. Dubernard, "Transrectal high-intensity focused ultrasound: minimally invasive therapy of localized prostate cancer", Journal of Endourology **14**, 519–528 (2000).

[5] J. Kennedy, F. Wu, G. Ter Haar, F. Gleeson, R. Phillips, M. Middleton, and D. Cranston, "High-intensity focused ultrasound for the treatment of liver tumours", Ultrasonics **42**, 931–935 (2004).

[6] D. Gianfelice, A. Khiat, M. Amara, A. Belblidia, and Y. Boulanger, "Mr imaging–guided focused us ablation of breast cancer: Histopathologic assessment of effectiveness—initial experience", Radiology **227**, 849–855 (2003).

[7] R. Illing and A. Chapman, "The clinical applications of high intensity focused ultrasound in the prostate", International Journal of Hyperthermia **23**, 183–191 (2007).

[8] I. Rivens, A. Shaw, J. Civale, and H. Morris, "Treatment monitoring and thermometry for therapeutic focused ultrasound", International journal of hyperthermia **23**, 121–139 (2007).

[9] J. Kennedy, "High-intensity focused ultrasound in the treatment of solid tumours", Nature Reviews Cancer **5**, 321–327 (2005).

[10] C. Coussios, C. Farny, G. Ter Haar, and R. Roy, "Role of acoustic cavitation in the delivery and monitoring of cancer treatment by high-intensity focused ultrasound (hifu)", International Journal of Hyperthermia **23**, 105–120 (2007).

[11] A. Welch, *Optical-thermal response of laser-irradiated tissue* (Springer Verlag) (2010).

[12] S. Thomsen, S. Jacques, and S. Flock, "Microscopic correlates of macroscopic optical property changes during thermal coagulation of myocardium", in *Proceedings of SPIE*, volume 1202, 2 (1990).

[13] A. Nilsson, C. Sturesson, D. Liu, and S. Andersson-Engels, "Changes in spectral shape of tissue optical properties in conjunction with laser-induced thermotherapy", Applied optics **37**, 1256–1267 (1998).

[14] P. Lai, J. McLaughlan, A. Draudt, T. Murray, R. Cleveland, and R. Roy, "Real-time monitoring of high-intensity focused ultrasound lesion formation using acousto-optic sensing", Ultrasound in Medicine & Biology (2011).

[15] S. Powell and T. Leung, "Acousto-optic monitoring of high-intensity focused ultrasound lesion formation with fibre-coupled autocorrelation detection", The Journal of the Acoustical Society of America **131**, 3210–3210 (2012).

[16] U. Vyas and D. Christensen, "Extension of the angular spectrum method to calculate pressure from a spherically curved acoustic source", Journal of the Acoustical Society of America **130**, 2687–2693 (2011).

[17] J. Douglas and H. Rachford, "On the numerical solution of heat conduction problems in two and three space variables", Trans. Amer. Math. Soc **82**, 421–439 (1956).

[18] H. Pennes, "Analysis of tissue and arterial blood temperatures in the resting human forearm", Journal of applied physiology **1**, 93–122 (1948).

[19] Q. Fang and D. Boas, "Monte carlo simulation of photon migration in 3d turbid media accelerated by graphics processing units", Optics express **17**, 20178–20190 (2009).

[20] S. Sapareto and W. Dewey, "Thermal dose determination in cancer therapy", International Journal of Radiation Oncology* Biology* Physics **10**, 787–800 (1984).

[21] J. Pearce, “Relationship between arrhenius models of thermal damage and the cem 43 thermal dose”, in *Proceedings of SPIE*, volume 7181, 718104 (2009).

[22] S. Sakadžić and L. Wang, “Correlation transfer equation for ultrasound-modulated multiply scattered light”, Physical Review E **74**, 036618 (2006).

[23] S. Powell and T. Leung, “Highly parallel monte-carlo simulations of the acousto-optic effect in heterogeneous turbid media”, Journal of Biomedical Optics **17**, 045002–1 (2012).